SEGMENTATION OF BIOMEDICAL IMAGES WITH EIGENVECTORS

Achilleas S. Frangakis, Reiner Hegerl

Max Planck Institut für Biochemie
Am Klopferspitz 18a, 82152 Martinsried
Germany
e-mail: frangak@biochem.mpg.de

ABSTRACT

We propose the use of eigenvectors for automated multidimensional image segmentation. The approach of Shi and Malik [8] has been extended in three dimensions and applied on biomedical data from electron microscopy and electron beam computed tomography. The approach exploits different similarity criteria e.g. proximity and gray level similarity. Theory, implementation, parameter setting and results are discussed in detail. The method turns out be a powerful tool for visualization, with the potential for developing further affinity measurements adapted to specific applications.

1. INTRODUCTION

Image segmentation techniques can be classified into two broad families: the contour-based and the region-based approaches. Contour-based approaches usually start with a local edge detection step, followed by a linking process towards a detectable boundary. Region-based approaches try to find partitions to the image pixels into sets corresponding to coherent image properties. The major difference between these techniques is the decision criterion: local vs. global. Contour-based techniques make local decisions (e.g. merge/split, stop/evolve). Region-based techniques make the decision by defining a global objective function [5]. The advantage thereby is that decisions are made by taking into account the information from the whole image.

In biomedical images the object of interest is usually a small feature, compared to the whole image e.g. molecule, tumor. This object needs to be segmented, but has always to be investigated in the total context. In case of structural information available, e.g. a gray value fingerprint, one can search specifically for this feature by some similarity measurement algorithms [3]. In pleomorphic, dynamically changing objects, - as the majority of the investigated specimens - size and shape are not known, but nevertheless characterized by a boundary or gray value variation. In the high-end tasks as electron microscopy or electron beam computed tomography the low signal to noise ratio hinders the segmentation procedure significantly, due to the fact that these techniques push the resolution to the cutting edge in the space and in the time domain.

The traditional method of object separation is histogram thresholding, commonly used for surface rendering. Unfortunately in images with band-pass characteristic no clear cut set of the histogram peaks correspond to distinct objects in the image. The use of eigenvectors for segmenting 2D and 3D images is a new and exciting approach in this field [8]. The resulting image has a gray value characteristic, which allows the segmentation of distinct features by automated methods or by histogram thresholding. The segmentation occurs stepwise in an hierarchical order such that in each step a dominant feature is separated from the rest by minimizing a parameter defined cost-function-

The paper is organized in the following way: In the next section a small review of the algorithm and the implementation in 3D is presented. In section III the segmentation of 2D and 3D images will be presented and the performance of the algorithm will be evaluated.

2. ALGORITHM

Graph theoretical approach

The image is considered as a weighted, undirected graph, where each pixel corresponds to a node and an edge is formed between every pair of nodes. The weight $w(i, j)$ of each edge is a function of the similarity between nodes i and j. Shi and Malik suggested to minimize the extension of the cut criterion $cut(A,B) = \sum_{u \in A, v \in B} w(u,v)$ namely the *normalized-cut*:

$$Ncut(A,B) = \frac{cut(A,B)}{asso(A,V)} + \frac{cut(B,A)}{asso(B,V)}, \qquad (1)$$

with $asso(A,V) = \sum_{u \in A \cap B} \sum_{v \in A} w(u,v)$, in order to separate the image in two pixel groups A and B [6]. The new criterion avoids the segmentation of separated nodes and improve the segmentation result.

Affinities

The affinity matrix **W** contains the similarity values $w_{i,j}$ connecting two nodes *i* and *j*, affiliated from some similarity criteria, as proximity, gray value, energy and texture. In our applications in electron microscopic images (in 2D and 3D) as well as in EBCT, texture regions are not so widespread and energy measurements require significant amounts of memory. Therefore the pixel value of the affinity matrix is the product of two components: the weight component $w_I(i,j)$ as a function of the gray values I_i

$$w_I(i,j) = \exp\left(-\left(I_i - I_j\right)^2 / a_I\right), \qquad (2)$$

and the proximity component $w_d(i,j)$ as the function of the Euclidean distance $d(x_i, x_j)$:

$$w_d(i,j) = \exp\left(-d(x_i, x_j)^2 / a_d\right), \qquad (3)$$

where a_I and a_d denote the gray value affinity variable the distance affinity variable, respectively.

Segmentation procedure

Shi and Malik proved that the solution for the minimization of the *Ncut* can be approximated by the second smallest eigenvector of a suitably normalized affinity matrix (SM algorithm). This statement coincidences with the theorem of Fiedler [1]. A different approach from Scott and Longuet-Higgins (SLH) uses a number of the smallest eigenvectors, nevertheless with a not normalized affinity matrix [7]. Y. Weiss proved that the combination of both algorithms by using the normalized affinity as proposed by SM and *k* eigenvectors as proposed by SLH produces the best result [11]. In our further experiments we will make use of this combined algorithm.

Implementation of the algorithm

The implementation of the algorithm is not trivial, due to the huge amount of data to be handled, especially in three dimensions. The affinity matrix **W** possesses N^2 elements ($\dim(N,N)$), where N is the number of pixels/voxels in the image that should be segmented. Handling with such large matrices would make the algorithm totally useless due to the huge amount of memory resources needed. With windowing (window of width *R*) of the weighting components the number of the elements of the affinity matrix reduces to $N \cdot R^2$ elements in 2D images and $N \cdot R^3$ in 3D images. In this case a sparse matrix representation is possible and the number of elements handled is acceptable. The calculation of the few first eigenvectors is then performed with the Lanczos algorithm [9], which exists in a parallelized version with the MPI interface. Realization of this algorithm allows reducing the memory resources, with faster computation times.

In general after the first calculation of the eigenvectors the desired feature is not perfectly segmented. In this case the first eigenvector is separated in two parts, usually by some threshold scheme and the segmentation procedure is applied again to each part separately [11].

Noise performance

Eigenvector analysis is commonly used in the multivariate statistical analysis and is known as a noise robust tool, which becomes effective in the case of analyzing multiple realizations of the objects under scrutiny. In the segmentation context, there is only a single realization of the image, which does not allow to classify the signal against the noise in a statistical manner. This yields to process every pixel as a signal assuming thereby that it is noise-free. This observation clarifies that a denoising algorithm needs to be applied prior to the segmentation. Nevertheless in the eigenvector approach the remaining spurious noise features do not contribute significantly to the segmentation result, at least in the first segmentation steps,.

3. SEGMENTATION RESULTS

Two-dimensional segmentation

The first example presents the performance of the segmentation on 2D images from a tomographic reconstruction of a *Pyrodictium abyssi* cell (Fig. 1a). The segmentation separates nicely the cell from the extracellular vesicles obtained on the right side of the image and also from the canulla. In order to support the segmentation result, the image has been first denoised with nonlinear anisotropic diffusion (Fig. 1b) [2].

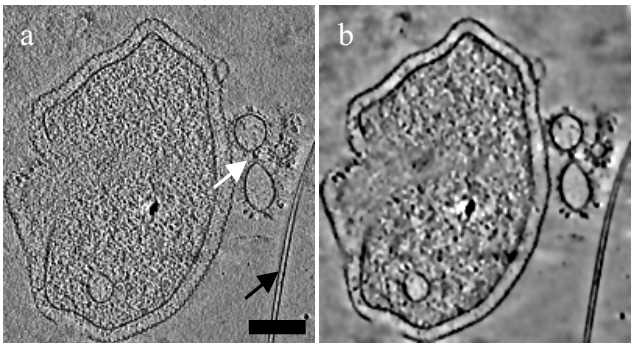

Fig. 1. Slice through an electron tomographic reconstruction of a *Pyrodictium abyssi* cell; (a) original slice and (b) slice denoised by nonlinear anisotropic diffusion. The white arrow points to the extracellular vesicles and the black arrow points to the canulla. The scale bar corresponds to 20 nm.

The vector containing the segmentation information possesses bright gray values at the place, where the cell lies and is darker everywhere else (Fig. 2a). The cell can than be separated from the rest of the environment with a simple thresholding scheme. The contour of the cell is precisely defined. In order to separate the extracellular vesicles from the canulla and the background a new segmentation cycle needs to been initialized. By further segmenting of the cell its boundary (S-layer) can be separated as an independent feature (white and black lines in Fig. 2b, c, d, e).

A new and promising development arising from classical X-ray tomography is "electron beam computed tomography (EBCT)". It is the fast alternative to computed X-ray tomography (CT) in medical imaging. A full 3D data set can be recorded in 50-100 msec, which allows for time-sensitive investigations, such as examination of a heart with very little motion artifacts [10]. However, in comparison to standard or helical CT data the SNR is considerably decreased, which prevents the application of automatic segmentation techniques for extraction of anatomical contours. In the following example a slice through the 3D image is segmented, showing a slice through the heart, lounge and aorta (Fig. 3a). After applying the segmentation procedure every single part of the image is segmented (Fig. 3b).

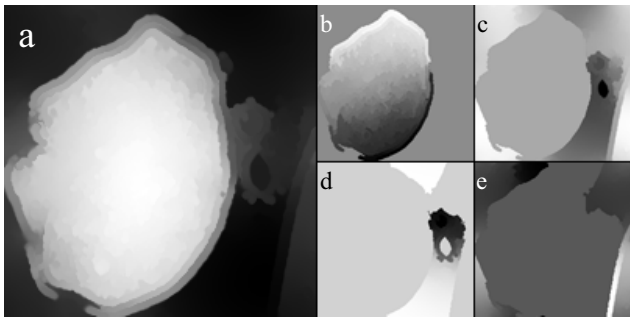

Fig. 2. Segmentation results of the *Pyrodictium abyssi* cell; (a) the original second smallest eigenvector as produced from the combination of the SLH and SM algorithms. (b) Further segmentation of the bright values. In white and black the boundary (S-layer) of the cell is coded. (c) Segmentation of the darker values. The extracellular vesicles get separated from the ice, the canulla and the background. (d) Final segmentation of the extracellular vesicles. (e) final segmentation of the canulla.

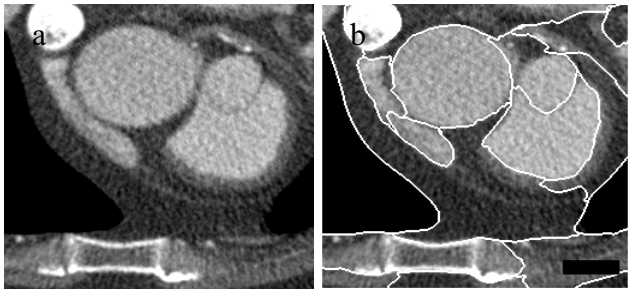

Fig. 3. Slice through the EBCT data; (a) original slice and (b) segmentation result. The scale bar corresponds to 5 cm

Segmentation of 3D images

The segmentation procedure can be directly applied on 3D data, with similar results. Nevertheless in electron tomographic reconstructions the specimen can not by tilted for high angles, due to mechanical reasons, resulting to an incomplete information. This effect hinders the segmentation significantly by smoothing all gray level gradients in the direction parallel to the illumination beam [4]. This effect, which effectively eliminates all the gray value gradients in the z-direction hinders a segmentation significantly. We have applied several algorithms on this type of data, e.g. level sets [6], and they mainly fail due to this effect. Unfortunately a correction is not possible due to physical reasons. This causes an effect of an anisotropic blurring, which is equivalent to a slower change of information in the z-direction. For this reason the 3D window for collecting the values can be chosen anisotropically or the number of slices used for the segmentation in the z-direction can be reduced. In the next examples the first option has been used.

The electron tomographic reconstruction of viruses attached to vesicles is an example for 3D segmentation with eigenvectors. In order to improve the visualization the carbon film was separated from the rest. Additionally the vesicles could be also removed in order to investigate the viruses only. In this way a view from the "down" side of the 3D image is possible.

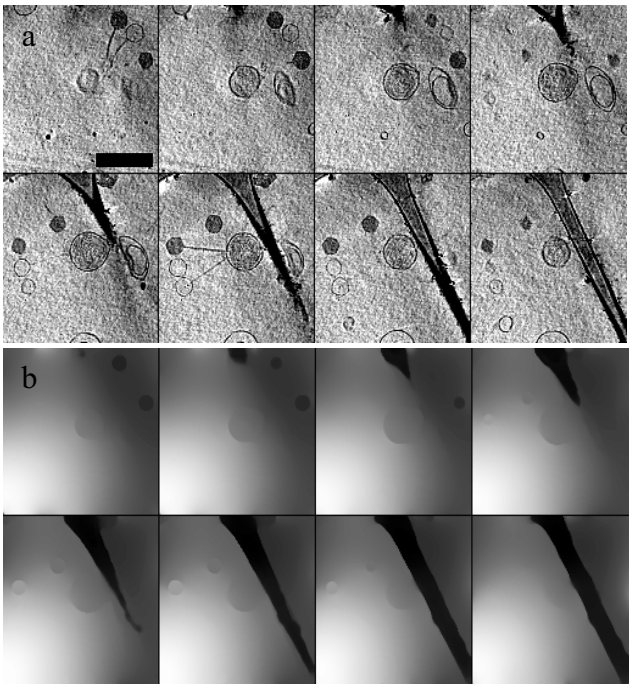

Fig. 4. Slices from the original tomographic reconstruction of T5 viruses attached to vesicles. In the center of the 3D image a vesicle can be observed with DNA inside, which has been

injected by the six viruses attached. (a) Original reconstruction, (b) segmentation result. The carbon foil presented in the center can now be removed easily from the image. The scale bar corresponds to 80 nm

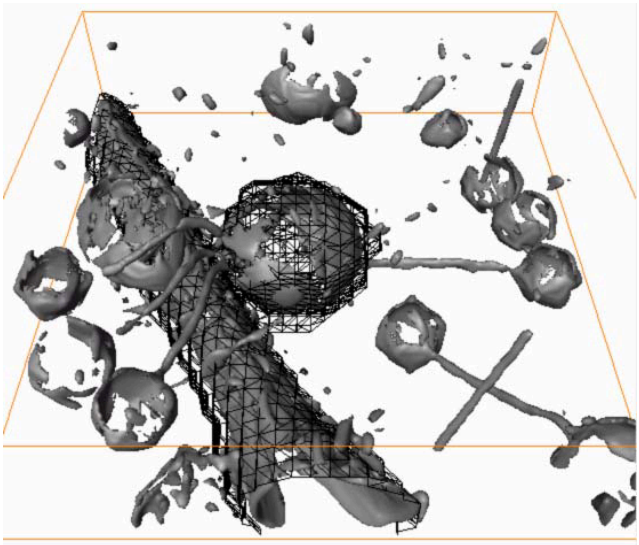

Fig.5 Isosurface representation of the vesicle with the viruses attached. In the wire-frame representation the segmented features are presented. The carbon foil in the center and the vesicles can than be separated.

4. DISCUSSION

The segmentation with eigenvectors proved to be an excellent segmentation tool for biomedical images. The similarity measurements can be freely chosen, giving great flexibility. Additionally it turned out that the parameter setting is very robust, as in our tested images the segmentation result was satisfying without any parameter modification. For 3D segmentation of electron microscopic images the influence of the incomplete data affects the result, nevertheless the performance remains superior to any other tested technique.

REFERENCES

[1] M .Fiedler, “A property of Eigenvectors of nonnegative symmetric matrices and its application to graph theory”, 1975, *Czechoslovak Mathematical Journal*, vol. 25, pp.619-633

[2] A. S. Frangakis, A. Stoschek, R. Hegerl, “Wavelet transform filtering and nonlinear anisotropic diffusion assessed for signal reconstruction performance on multidimensional biomedical data”, *IEEE Trans. Biomedical Engineering*, vol. 48, no. 2, pp. 213-222

[3] A. S. Frangakis, J. Böhm, D. Nicastro, S. Nickell, F. Förster, R. Hegerl, W. Baumeister “Automated identification of macromolcular complexes in electron tomograms of cells”, submitted to *PNAS*

[4] A. J. Koster, R. Grimm, D. Typke, R. Hegerl, A. Stoschek, J. Walz, and W Baumeister, “Perspectives of molecular and cellular electron tomography”, *J. of Structural Biology*, vol. 120, pp. 276-308, 1998

[5] J. Malik, S. Belognie, T. Leung, J Shi, ”Contour and texture analysis for image segmentation”, 1999, submitted to *Int. J. Comp. Vision*

[6] R. Malladi, J. Sethian, B. C. Vemuri, “A fast level set based algorithm for topology –independent shape modeling”, “Journal of Mathematical Imaging and Vision”, 1996, vol. 6, pp. 269-28

[7] G.L. Scottt and H. C. Longuet-Higgins, “Feature grouping by relocalisation of eigenvectors of the proximity matrix”, *Proc. British Machine Vision Conf.*, 1990, pp. 103-108

[8] J. Shi and J. Malik, “Normalized cuts and image segmentation”, *Proc. IEEE Conf. on Comp. Vision and Pattern Recognition*, 1997, pp. 731-737

[9] D. C. Sorensen, “Implicitly restarted Arnoldi/Lanczos methods for large scale eigenvalue calculations”, 1995, technical report

[10] S. Wang, R. Detrano, A. Secci, W. Tang, T. Doherty, G. Puentes, N. Wong, B. Brundage, "Detection of coronary classification with electron-beam computed tomography: Evaluation of interexamination reproducibility and comparison of three image acquisition-protocols", 1996, *Amer. Heart J.*, vol. 132, no. 3, pp.550-558

[11] Y. Weiss, “Segmentation using eigenvectors: a unifying view”, *Proc. Int. Conf. Comp. Vision*, 1999, vol.2, pp. 975-982